

Experimental Study of the Thermal Transport in CsNiF₃ — An $S = 1$ Quantum Chain

V. TKÁČ^a, A. ORENDÁČOVÁ^a, M. ORENDÁČ^a, D. LEGUT^b, K. TIBENSKÁ^c, A. FEHER^a,
M. POIRIER^d AND M.W. MEISEL^e

^aCentre of Low Temperature Physics, Faculty of Science, P.J. Šafárik University
Park Angelinum 9, 041 54 Košice, Slovakia

^bInstitute of Physics of Materials, Academy of Sciences of the Czech Republic
Žižkova 22, CZ-616 62 Brno, Czech Republic

^cFaculty of Aeronautics, Technical University, Rampová 7, 041 21 Košice, Slovakia

^dRegroupement Québécois sur les Matériaux de Pointe, Département de Physique, Université de Sherbrooke
Sherbrooke, Québec J1K 2R1, Canada

^eDepartment of Physics and the National High Magnetic Field Laboratory, University of Florida
Gainesville, Florida 32611-8440, USA

The heat transport in a single-crystal of CsNiF₃ has been performed in the temperature range from 2 K to 7 K in a zero magnetic field, $B = 0$, as well as in sufficiently large magnetic fields, $B = 6$ T and 9 T, inducing the ferromagnetic ground state along the hard c -axis. CsNiF₃ represents an $S = 1$ quasi-one-dimensional XY ferromagnet with the intra-chain exchange coupling $J/k_B \approx 24$ K, single-ion anisotropy $D/k_B \approx 8$ K, and ordering temperature $T_N = 2.7$ K. Comparison of the phonon and magnon velocities suggests that phonons are the main heat carriers in this magnetic insulator. The thermal conductivity in $B = 0$ was analysed in the frame of a standard Debye model. The temperature dependence of the effective phonon mean free path was calculated from the experimental data, and the enhancement of the phonon mean free path in $B \neq 0$ was obtained, indicating that magnons act as scattering centers for phonons.

PACS: 75.30.Et, 75.40.Cx, 66.70.Lm, 75.30.Ds

1. Introduction

In recent years, the theoretical and experimental investigation of heat transport in low-dimensional spin systems experienced a renaissance because of the progress in the theory of anomalous heat transport in low-dimensional magnets [1]. One interesting example is CsNiF₃, a quasi-one-dimensional $S = 1$ planar ferromagnet with intra-chain exchange interaction $J/k_B \approx 24$ K, single-ion anisotropy $D/k_B \approx 8$ K, and long-range antiferromagnetic ordering temperature $T_N = 2.7$ K. With an extensive history [1–4] that continues to evolve [5–7], CsNiF₃ was originally considered as a model soliton-bearing system [4], but subsequent theoretical studies showed that the magnetism is well-described by spin-wave theory [6, 8]. Previous investigations of the thermal transport, performed in magnetic fields applied in the easy plane and thus supporting the formation of magnetic solitons, indicated the presence of phonon–magnon scattering and the absence of an effect from the solitons [9]. The present work involves the analysis of the

heat transport in CsNiF₃ studied in zero magnetic field as well as in finite magnetic fields applied perpendicular to the easy plane.

2. Experimental details

CsNiF₃ crystallizes in the hexagonal space group $P6_3/mmc$ with two formula units per unit cell where $a = 6.255$ Å and $c = 5.242$ Å [10]. Between 2 K and 7 K and in magnetic fields of $B = 0.6$ T, and 9 T, the temperature dependence of the thermal conductivity was measured using a standard steady-state heat-flow method with two heaters coupled to a special sample holder [11]. The magnetic fields and the heat flow were both applied along the magnetic chains running parallel to the c -axis, which is perpendicular to the easy plane. The thermometers were corrected for magnetoresistance effects. The experimental sample was a single crystal of irregular shape, with approximate dimensions $1.2 \times 0.75 \times 12$ mm³, that was light green and transparent with some internal cleavage planes visible. Prior to mounting, the sample was

continuously kept in paraffin oil because of its highly hygroscopic nature.

3. Results and discussion

The temperature dependence of the thermal conductivity of CsNiF₃ is shown in Fig. 1, and monotonic behavior was observed in all fields. The effect of magnetic field on the heat transport is evident, as the thermal conductivity increases with increasing magnetic field over the entire temperature range.

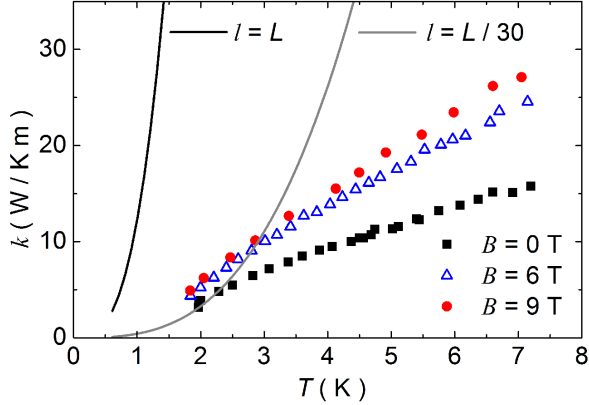


Fig. 1. Temperature dependence of the thermal conductivity of CsNiF₃ in magnetic fields $B = 0, 6,$ and 9 T. The solid lines represent the theoretical predictions from kinetic theory of gases when $l = L = 7.5 \times 10^{-4}$ m, the shortest dimension of the sample, and $l = L/30$ (see text).

Since CsNiF₃ is a magnetic insulator, phonons and magnetic excitations can be considered as heat carriers. To identify the contribution of the lattice and magnetic subsystems to the heat transport, the velocities, v , of the phonons and the magnons in zero magnetic field have been estimated. The former has been calculated using the values of elastic constants determined from the ultrasonic experiments at 300 K [12] and a Voigt–Reuss–Hill averaging procedure [13], yielding estimates for the bulk and shear modulus for an isotropic (polycrystalline) system of $B = 30$ GPa and $G = 10.9$ GPa. The density of CsNiF₃ is 4.648 g/cm³ [10], so the velocities parallel and perpendicular to the chains are, respectively, $v_{\parallel} = \sqrt{(B + 4G/3)/\rho} = 3.3 \times 10^3$ m/s and $v_{\perp} = \sqrt{G/\rho} = 1.5 \times 10^3$ m/s. Following the approach described in Ref. [14], the average value of the phonon velocity, weighted in favor of the transverse modes as the dominant heat carriers at low temperatures, is $v_{\text{ph}} = 1.6 \times 10^3$ m/s, as calculated according to $v = v_{\parallel} \frac{2s^2+1}{2s^3+1}$, where $s = \frac{v_{\parallel}}{v_{\perp}}$ represents a ratio of the longitudinal and transverse phonon velocities. The corresponding Debye temperatures $\Theta_{\text{D}}^{\parallel} = 355$ K and $\Theta_{\text{D}}^{\perp} = 175$ K were calculated using the equation $\Theta_{\text{D}} = v_{\text{ph}} \sqrt[3]{6\pi^2 n}/k_{\text{B}}$, where n represents the number density of atoms. These values are comparable to those obtained from the lattice

specific heat [15], and in the forthcoming analysis, the average value, $\Theta_{\text{D}} \approx 235$ K, will be used.

With respect to the magnon velocities, the intra-chain magnon group velocity was estimated by differentiating the magnon dispersion spectrum [8] describing the magnetic excitation spectrum of CsNiF₃ in its $B = 0$ paramagnetic phase. Using the aforementioned J and D values, the magnon velocity was evaluated near the vicinity of the Brillouin zone center, $v_{\text{m}} = \left. \frac{d\omega}{dq} \right|_{q=0} \approx 3 \times 10^3$ m/s. Obviously the intra-chain magnon velocity is comparable with the phonon velocity, so both channels might contribute to the heat transport in CsNiF₃. However, most of the experimental data are taken at temperatures above the phase transition, where only short-range magnetic order is formed. Nevertheless, the temperature dependence of the density of correlated spins in the paramagnetic phase can be estimated [16], and a non-negligible number of correlated spins exist at temperatures up to about 20 K. On the other hand, the finite extent of these short-range correlated regions at these temperatures prevents the undamped propagation of the long wavelength spin waves. Thus, despite their large velocity, magnons cannot represent an effective channel for the heat transport and will only act as scattering centers for phonons that can be treated as the main heat carriers in CsNiF₃.

The contribution of phonons to the thermal conductivity, k , can be evaluated from the kinetic theory of gases, which gives $k = \frac{1}{3} C v l$, where C represents the lattice specific heat, v is average phonon velocity, and l is the phonon mean free path. Using the lattice specific heat from Ref. [14], the aforementioned average phonon velocity, v_{ph} , and $l = L = 7.5 \times 10^{-4}$ m, the shortest dimension of the sample, the phonon thermal conductivity was calculated and is shown in Fig. 1. In addition, a significantly shorter mean free path, $l = L/30$, which may arise from the microscopic defects in the crystal, was also used to demonstrate the dramatic differences between the simple expectation and the data.

Another way to see this result is to consider the temperature dependence of the phonon mean free path, $l = \frac{3k}{Cv}$, shown in Fig. 2, which indicates the presence of other phonon scattering mechanisms even at the lowest temperatures. Indeed, the magnetic subsystem represents another source of scattering that is manifested by the enhancement of the mean free path in applied magnetic field over the entire temperature range. To include other scattering mechanisms, a standard Debye model with the relaxation time approximation [14] was applied to describe the behavior of the thermal conductivity in zero magnetic field, yielding

$$k = \frac{k_{\text{B}}}{2\pi^2 v} \left(\frac{k_{\text{B}}}{\hbar} \right)^3 T^3 \int_0^{\frac{\Theta_{\text{D}}}{T}} \tau(x) \frac{x^4 e^x}{(e^x - 1)^2} dx, \quad (1)$$

where $x = \frac{\hbar\omega}{k_{\text{B}}T}$ and τ represents a total relaxation time. The form of Eq. (1) assumes the same phonon velocity for all three polarizations, so the aforementioned average value of the phonon velocity and the Debye temper-

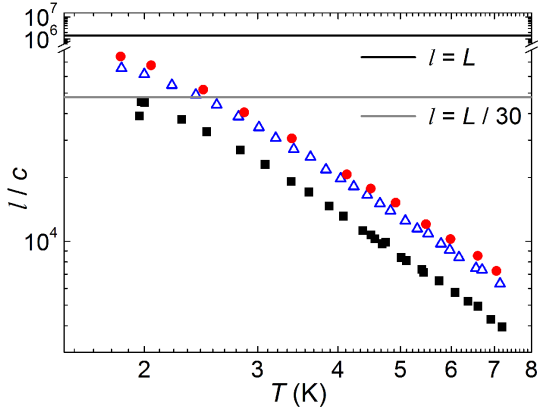


Fig. 2. The temperature dependence of the phonon mean free path, l , in $B = 0$ (full squares), $B = 6$ T (triangles), and $B = 9$ T (circles). The limits of $l = L$ and $l = L/30$ are also shown. All values are normalized by the lattice constant c , and the temperature scale is logarithmic.

ature were used in the analysis. As can be seen from Fig. 2, the application of a magnetic field does not remove the discrepancy between the data and the limiting value of the phonon mean free path at the lowest temperatures, so structural defects and other scattering processes are clearly reducing the phonon path length. Consequently, as a first step, a simplified model was used and included phonon boundary scattering represented by the relaxation time, $\tau_{\text{bd}}^{-1} = \frac{v_{\text{ph}}}{L}$, the scattering on point defects, $\tau_{\text{pt}}^{-1} = P\omega^4$, and umklapp processes, $\tau_{\text{um}}^{-1} = UT\omega^3 e^{-\frac{\Theta_D}{uT}}$ [17], where U , u , and P are phenomenological parameters and where the total relaxation time was calculated as $\tau^{-1} = \tau_{\text{bd}}^{-1} + \tau_{\text{um}}^{-1} + \tau_{\text{pt}}^{-1}$.

However, this simplified model does not adequately describe the behavior of the thermal conductivity (Fig. 3), so other structural defects were taken into account. The scattering by dislocations, $\tau_{\text{dis}}^{-1} = D\omega^3$, and the strain fields of dislocations, $\tau_{\text{str}}^{-1} = N\omega$, were added to the model, where N and D are parameters given by the concentration of dislocation lines [14]. With the total relaxation time $\tau^{-1} = \tau_{\text{bd}}^{-1} + \tau_{\text{um}}^{-1} + \tau_{\text{pt}}^{-1} + \tau_{\text{dis}}^{-1} + \tau_{\text{str}}^{-1}$, the fitting procedure yielded reasonable values for the parameters [17]. Finally, it is noteworthy that the inclusion of the scattering on dislocations significantly improved the agreement between the model and the experimental data (Fig. 3).

4. Conclusion

Although the magnon and phonon velocities in CsNiF_3 have been estimated to have similar values, the analysis of the thermal conductivity indicates that magnons act as phonon scattering centers due to the damping in the paramagnetic phase. These results, together with the calculated phonon mean free path, suggest that phonons are the main heat carriers in CsNiF_3 . The applica-

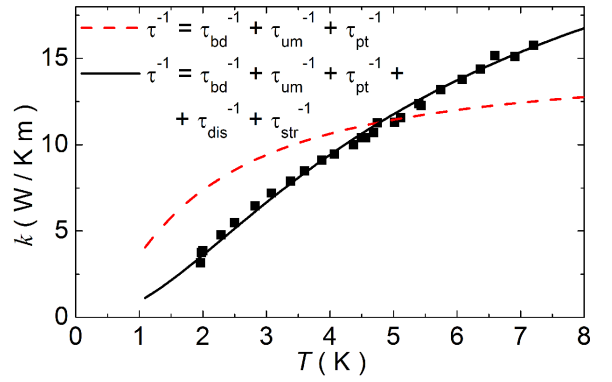


Fig. 3. Temperature dependence of the thermal conductivity of CsNiF_3 in zero magnetic field (squares) and theoretical predictions obtained from standard Debye model. The dashed line represents the model, where boundary scattering, umklapp scattering, with $u = 1.5$ and $U = 2.3 \times 10^{-28} \text{ s}^2 \text{ K}^{-1}$, and point defect scattering, with $P = 7.7 \times 10^{-41} \text{ s}^3$, were included. The solid line represents the model, where boundary scattering, umklapp scattering, with $u = 1.5$ and $U = 5.1 \times 10^{-29} \text{ s}^2 \text{ K}^{-1}$, point defect scattering, with $P = 1.1 \times 10^{-41} \text{ s}^3$, scattering on core of dislocations, with $D = 1.1 \times 10^{-31} \text{ s}^3$, and scattering on strain fields of dislocations, with $N = 3.8 \times 10^{-5} \text{ s}$, were included. All calculations were performed for $L = 7.5 \times 10^{-4} \text{ m}$, $v_{\text{ph}} = 1.6 \times 10^3 \text{ m/s}$, and $\Theta_D \approx 235 \text{ K}$.

tion of a magnetic field did not significantly enhance the phonon mean free path, indicating the dominance of phonon scattering from structural defects and other mechanisms within the phonon subsystem. The analysis of the thermal conductivity within a Debye model using a relaxation-time approximation yielded a good description of the experimental data. Detailed analysis of the thermal conductivity in nonzero magnetic field will be a subject of future studies.

Acknowledgments

This work has been supported by VEGA grant 1/0078/09, project APVT-0006-07, NSF DMR-0701400 (MWM), NSF DMR-0654118 (NHMFL), and ERDF EU project No. ITMS26220120005. Financial support from US Steel DZ Energetika is greatly acknowledged.

References

- [1] A.V. Sologubenko, H.R. Ott, in: *Strong Interactions in Low Dimensions*, Eds. D. Baeriswyl, L. Degiorgi, Kluwer Academic Publishers, Dordrecht 2004, p. 383.
- [2] L.J. de Jongh, A.R. Miedema, *Adv. Phys.* **23**, 1 (1974).
- [3] M. Steiner, J. Villain, C.G. Windsor, *Adv. Phys.* **25**, 87 (1976).
- [4] H.-J. Mikeska, M. Steiner, *Adv. Phys.* **40**, 191 (1991).

- [5] M. Orendáč, A. Orendáčová, E. Čížmár, J.-H. Park, A. Feher, S.J. Gamble, S. Gabáni, K. Flachbart, J. Karadamoglou, M. Poirier, M.W. Meisel, *Phys. Rev. B* **69**, 184403 (2004).
- [6] V. Lisý, J. Tóthová, *Acta Phys. Pol. A* **118**, 953 (2010).
- [7] D. Legut, U.D. Wdowik, *J. Phys. Condens. Matter* **22**, 435402 (2010).
- [8] J. Karadamoglou, N. Papanicolaou, X. Wang, X. Zotos, *Phys. Rev. B* **63**, 224406 (2001).
- [9] H.A.M. de Gronckel, W.J.M. de Jonge, K. Kopinga, L.F. Lemmens, *Phys. Rev. B* **44**, 4654 (1991).
- [10] R.E. Schmidt, M. Welsh, S. Kummer-Dörner, D. Babel, *Z. Anorg. Allg. Chem.* **625**, 637 (1999).
- [11] A. Orendáčová, K. Tibenská, E. Čížmár, M. Orendáč, A. Feher, *Cryogenics* **47**, 61 (2007).
- [12] F. Ganot, P. Moch, J. Nouet, *J. Magn. Magn. Mater.* **31-34**, 1165 (1983).
- [13] O.L. Anderson, *J. Phys. Chem. Solids* **24**, 909 (1963).
- [14] R. Berman, *Thermal Conductivity in Solids*, Clarendon Press, Oxford 1976.
- [15] J.V. Lebesque, J. Snel, J.J. Smith, *Solid State Commun.* **13**, 371 (1973).
- [16] Ch. Rosinski, B. Elschner, *J. Magn. Magn. Mater.* **4**, 193 (1977).
- [17] A.V. Sologubenko, K. Gianno, H.R. Ott, U. Ammerahl, A. Revcolevschi, *Phys. Rev. Lett.* **84**, 2714 (2000).